

Supporting Information

**Molecular Recognition of the Hybrid-2 Human Telomeric
G-Quadruplex by Epiberberine: Insights into Conversion of Telomeric
G-Quadruplex Structures**

*Clement Lin, Guanhui Wu, Kaibo Wang, Buket Onel, Saburo Sakai, Yong Shao, and
Danzhou Yang**

anie_201804667_sm_miscellaneous_information.pdf

Supporting Information

Table of Contents

1. Experimental Procedures

a. DNA Sample Preparation	3
b. Nuclear Magnetic Resonance Spectroscopy Experiments	3
c. Complete Proton Resonance Assignment	4
d. NOE-distance restrained molecular dynamics calculations	4
e. Circular Dichroism (CD) Spectroscopy Experiments	5
f. Taq Polymerase Stop Assay	5
g. Native Gel Electrophoretic Mobility Shift Assay (EMSA)	6
h. Fluorescence Experiments	6

2. Supplementary Tables

a. Table S1: Proton chemical shifts of wtTel26 at 25 °C	7
b. Table S2: Proton chemical shifts of wtTel26 at 15 °C	8
c. Table S3: Proton chemical shifts of EPI at 25 °C	9
d. Table S4: Interresidue NOEs between the 5'-external G-tetrad and the EPI-A3 plane	10
e. Table S5: Interresidue NOEs between the EPI-A3 plane and the T2-T13-A15 triad and A21	11
f. Table S6: Interresidue NOEs between the T2-T13-A15 triad and the T1-T14 pair	12
g. Table S7: Distance constraints and structure statistics for the 1:1 EPI-wtTel26 complex in K ⁺	13

3. Supplementary Figures

a. Figure S1 : Schematic drawing of wild-type telomeric G4 folding topologies	14
b. Figure S2 : Chemical structures of protoberberine alkaloids	15
c. Figure S3 : Imino proton assignment for the 1:1 EPI-wtTel26 complex	16
d. Figure S4: T/H3 imino proton assignment for the 1:1 EPI-wtTel26 complex	17

e. Figure S5 : Assignment of wtTel26 and EPI in the 1:1 EPI-wtTel26 complex	18
f. Figure S6 : Observed exchange peaks in the 2D-NOESY spectrum of the 0.75:1 EPI-wtTel26 complex	19
g. Figure S7 : Stacked plot of the 2D NOESY spectrum showing syn-configuration DNA residues	20
h. Figure S8 : 1D ¹ H NMR spectrum of the free EPI	21
i. Figure S9 : The proton chemical shift differences between the bound (in 1:1 EPI-wtTel26 complex) and free wtTel26	23
j. Figure S10 : CD spectra and thermal melting curves of wtTel26	24
k. Figure S11 : Stereo view of the superimposed 15 final NMR structures and representative NMR structure	25
l. Figure S12 : The imino proton regions of the variable temperature ¹ H NMR spectra of the 1:1 wtTel26-EPI complex	26
m. Figure S13 : Expanded imino regions of the 2D-NOESY spectrum of the 1:1 EPI-wtTel26 complex showing cross-peaks of T2/H3	27
n. Figure S14: ¹ H NMR titration of EPI with various human telomeric DNA sequences of differing topology	28
o. Figure S15 : ¹ H NMR titration of EPI with various human promoter DNA sequences of differing topology	29
p. Figure S16 : CD spectra of the wtTel26-EPI complex in Na ⁺ and K ⁺ containing solution	30
q. Figure S17 : 1D ¹ H NMR titration of EPI to wtTel26 in 100 mM Na ⁺	31
r. Figure S18 : Native EMSA gel of free wtTel26 its complexes with EPI under varying salt conditions	32
s. Figure S19 : Fluorescence competition experiments of EPI binding with wtTel26 and dsDNA	33
4. References	34

Experimental Procedures

DNA Sample Preparation. Oligonucleotides were synthesized and purified as previously described ^[1] using commercially available reagents. NMR samples were prepared to a final concentration of 0.1–1 mM in 100 mM K⁺ solution at pH 7 and containing 90/10/% H₂O/D₂O. Oligonucleotides were heated to 95 °C for 5 min then cooled slowly to room temperature for G-quadruplex formation. DNA was quantified by UV/Vis spectroscopy at 260 nm using their calculated extinction coefficients. A 40 mM EPI stock solution was prepared in DMSO and titrated into the DNA solution to the desired concentrations for the complex samples.

Nuclear Magnetic Resonance Spectroscopy Experiments. NMR experiments were conducted using a Bruker DRX-600 spectrometer or an AV-800 spectrometer with cryoprobe. Experiments were performed using Watergate water suppression. 1D ¹H NMR spectra were collected at 25 °C using the Bruker DRX-600 spectrometer. Oligonucleotides were prepared with site-specific 6-10% incorporation of ¹⁵N-labeled guanine and thymine at each respective position ^[1]. Guanine H1 and thymine H3 protons are one-bond connected to N1 or N3 and unambiguously assigned using ¹⁵N-edited 1D GE-JRSE HMQC experiments.^[2] NOESY experiments with 50, 150, and 250 ms mixing times, TOCSY experiments with 30 and 80 ms mixing times, and COSY experiments were collected for the 0.75:1 and 1:1 EPI-wtTel26 complex in pH 7, 100 mM K⁺ solution at 5, 15, and 25°C in both water and D₂O.

Complete proton resonance assignment and integrations were achieved using the Sparky (UCSF) (See Supplementary Information). Distances between protons were assigned based on the nuclear Overhauser effect (NOE) crosspeaks integrated at 250-ms mixing time. Peak volumes were referenced using the thymine HMe-H6 distance (2.99 Å) with distance restraints limits set to

20% variance. Pseudo-atoms replaced unresolved protons with appropriate corrections for the measured distance.

Complete Proton Resonance Assignment. Assignment and integrations were achieved using the Sparky (UCSF). Starting from unambiguous assignments of the imino (H1/H3) and aromatic (H8/H6) protons obtained from labeled DNA, complete proton assignment of the wtTel26 in the 1:1 EPI-wtTel26 complex was achieved by the sequential assignment method (**Tables S1, S2**). Exchange peaks in the NOESY spectra between the free and bound wtTel26 of the 0.75:1 EPI-wtTel26 complex further corroborated the assignment (**Fig. S6**).

Protons of the free EPI molecule were assigned using ^1H NMR and NOESY (**Fig. S8, Table S3**). Protons of the bound EPI molecule were assigned using NOESY experiments of the 1:1 EPI-wtTel26 complex (**Fig. S5b, Table S3**). The EPI methoxy resonances (HA and HB) are isolated from the DNA protons and readily identifiable. They were assigned based on the chemical shifts and number of their respective intramolecular NOE connectivities. This led to the assignment of the H1, H13, H12, and H11 protons through HA and of the H4 and H51/H52 protons through HB. The EPI H61/H62 and H8 protons were identified by the intermolecular NOEs with the DNA bases at the binding site (**Tables S4-S5**).

NOE-distance restrained molecular dynamics calculations. Structure calculations were performed using NOE restrained simulated annealing calculations in the program XPLOR (version 3.851)^[3]. The starting model of the 1:1 wtTel26–EPI complex was constructed in Insight II 2000.1 (Accelrys, CA, USA) based on the previously determined free wtTel26 G-quadruplex structure and binding site conformations deduced from NOE data. EPI topology and parameter files were generated using PRODRG^[4]. The skewed bi-harmonic energy function was used for distance constraints from NOE data. 664 total distances were used in the NOE-

restrained dynamics calculations. The system was subjected to 1000 steps of energy minimization with force constants of $1 \text{ kcal/mol}\cdot\text{\AA}^2$ for all restraints. Dihedral angle restraints of $60 (\pm 35)^\circ$ and $240 (\pm 40)^\circ$ with a force constant of $10 \text{ kcal}\cdot\text{mol}^{-1}\cdot\text{rad}^{-2}$ were then applied to experimentally determined *syn* and *anti* nucleotides respectively. NOE and hydrogen bond force constants were scaled to the final values of 10 and $30 \text{ kcal}\cdot\text{mol}\cdot\text{\AA}^2$ respectively. The structures were then equilibrated at 1000 K for 20 ps. Subsequent restrained simulated annealing simulation was conducted with temperature reduced by 25 K/cycle with 1000 time steps of 2 fs/cycle until the temperature reached 100 K. Resulting structures were further subjected to 1000 steps of energy minimization. The 15 best structures, selected based on their minimal energy terms and number of NOE violations, were deposited in the Protein Data Bank (PDB ID: 6CCW)

Circular Dichroism (CD) Spectroscopy Experiments. Circular dichroism spectra were recorded using a Jasco-1100 spectropolarimeter (Jasco Inc., Easton, MD) equipped with a temperature controlled cell holder. Samples were prepared in 100 mM K^+ or Na^+ -containing phosphate buffer at DNA concentrations of $35 \mu\text{M}$. CD measurements were taken through a quartz cell with a 1 mm path length. Spectra were attained using three averaged scans between 230 and 330 nm at 25°C . The baseline was corrected by subtracting signal contributions from the buffer. T_m values were determined using CD melting experiments at 290 nm with a heating rate of $2^\circ\text{C}/\text{min}$ and 1 s response time between 20 and 95°C .

Taq Polymerase Stop Assay. This assay was performed as previously described^[51]. Primers (5'-TAATACGACTCACTATAGC) labeled with $\gamma\text{-}^{32}\text{P}$ were mixed with template DNA in equal molar amounts (5'-TCCAACCTATGTATACTTAGGGTTAGGGTTAGGGTTAGGGTTACATATCGATGAAATTGCTATAGTGAGTCGTATTA-3') and annealed by heating to 95°C for 5 min then cooling to room temperature. EPI and KCl were added at various concentrations and

incubated at room temperature for 3 hr. Primer extension was performed in a 20 μ L reaction containing 50 nM cassette, 2 mM dNTP, 0.5 U/ μ L *Taq* polymerase (NEB), 50 mM Tris (pH 7.4), 1 mM MgCl₂, and 5 mM DTT. Sequencing reactions were conducted using a Thermo Sequenase Cycle Sequencing Kit.

Native Gel Electrophoretic Mobility Shift Assay (EMSA). Native PAGE experiments were performed with a 1.5mm thick 10 \times 7 cm native gel containing 18% acrylamide (Acrylamide:Bis-acrylamide 29:1) in TBE buffer, pH 8.0, supplemented with 12.5 mM NaCl. G-quadruplex samples containing 0.18 nmol DNA were prepared in K⁺ or Na⁺ containing buffer (pH 7.0) in the absence and presence of EPI. DNA bands were visualized using GelRedTM staining.

Fluorescence Experiments. Fluorescence spectra were acquired with a FLSP920 spectrofluorometer (Edinburgh Instruments Ltd., Livingston, UK) at 18 \pm 1 $^{\circ}$ C, which was equipped with a temperature-controlled circulator (Julabo Labortechnik GmbH, Seelbach, Germany). Fluorescence was measured in a quartz cell with path length of 1 cm, using excitation wavelength of 377 nm^[6]. The titration experiments were carried out at EPI concentration of 0.5 μ M in 100 mM K⁺. DNA at the specified concentration was added into the EPI solutions, and the resulting solutions incubated for 15 min before fluorescence measurements were taken. For hTelG4-dsDNA competition experiments, a mixture solution of 0.5 μ M EPI and 1 μ M wtTel26 in 100 mM K⁺ was titrated with double-stranded DNA (dsDNA) (5'-GTGTTGACAGCAGCG : 5'-CGCTGCTGTCAACAC) at increasing concentrations from 1 μ M to 50 μ M. For dsDNA binding constant determination, 0.5 μ M EPI was titrated with the dsDNA in 100 mM K⁺. The apparent k_d was estimated using KaleidaGraph (Synergy Software, PA) fitting of a 1:1 binding model.

Table S1. Proton chemical shifts of wtTel26 in the 1:1 EPI-wtTel26 complex and the free wtTel26 in parentheses at 25 °C in pH 7, 100 mM K⁺.

Base	H1/H2/H3	HMe	H6/H8	H1'	H2', H2''	H3'	H4'	H5', H5'' **
T1	10.55*	1.52 (1.62)	7.14 (7.32)	5.74 (5.84)	1.58, 2.03 (1.94, 2.17)	4.30 (4.43)	3.82 (3.82)	4.15, 4.15
T2	10.61*	0.85 (1.33)	7.13 (6.96)	5.74 (5.65)	2.06, 2.13 (1.67, 2.03)	4.62 (4.42)	3.91 (3.89)	3.69, 3.74 (3.63, 3.63)
A3	7.96 (7.74)		7.96 (7.88)	6.41 (6.07)	1.84, 2.46 (2.17, 2.68)	4.82 (4.81)	4.03 (4.18)	4.35, 4.35 (3.57, 3.82)
G4	11.69 (11.58)		7.51 (7.38)	6.06 (5.98)	3.00, 3.34 (2.94, 3.43)	4.87 (4.89)	4.30 (4.38)	4.19, 4.26
G5	11.61 (11.81)		7.95 (7.89)	5.68 (5.72)	2.37, 2.59 (2.43, 2.64)	5.01 (5.00)	4.29 (4.29)	4.10, 4.19
G6	11.01 (10.93)		7.78 (7.75)	5.96 (5.96)	2.35, 2.44 (2.30, 2.37)	4.95 (4.96)	4.37 (4.38)	4.15, 4.15 (4.18, 4.18)
T7		1.77 (1.83)	7.55 (7.65)	6.15 (6.24)	2.09, 2.43 (2.19, 2.48)	4.74 (4.73)	4.25 (4.32)	4.02, 4.20 (4.04, 4.19)
T8		1.68 (1.73)	7.33 (7.41)	5.65 (5.73)	1.88, 2.10 (1.92, 2.15)	4.48 (4.57)	3.95 (4.00)	3.83, 3.94
A9	7.43 (7.50)		7.65 (7.67)	5.69 (5.64)	1.88, 2.52 (1.90, 2.42)	4.83 (4.86)	4.14 (4.18)	3.96, 4.09 (3.01, 3.57)
G10	11.01 (11.09)		7.20 (7.25)	5.96 (6.03)	3.60, 3.03 (3.70, 3.14)	4.63 (4.83)	4.27 (4.28)	4.12, 4.20
G11	10.87 (11.07)		7.36 (7.34)	5.70 (5.74)	2.51, 2.38 (2.56, 2.45)	4.88 (4.99)	4.12 (4.30)	4.11, 4.28
G12	11.52 (11.58)		7.77 (7.81)	5.70 (5.88)	2.50, 2.65 (2.34, 2.55)	5.02 (5.05)	4.32 (4.35)	4.35, 4.37
T13	12.65	1.56 (1.87)	7.20 (7.62)	5.79 (6.05)	2.00, 2.67 (2.23, 2.52)	4.94 (4.82)	4.03 (4.33)	4.17, 4.15
T14	10.46*	1.79 (1.63)	7.74 (7.32)	5.87 (5.91)	2.46, 2.94 (1.61, 2.06)	5.02 (4.71)	4.14 (4.18)	3.93, 3.93 (3.98, 3.98)
A15	8.00 (8.00)		8.43 (8.15)	6.41 (6.45)	2.31, 2.94 (2.82, 2.82)	4.87 (5.04)	4.31 (4.44)	4.47, 4.47 (4.11, 4.15)
G16	10.66 (11.16)		7.55 (7.12)	6.10 (5.92)	3.09, 3.58 (2.91, 3.38)	4.73 (4.94)	4.22 (4.26)	4.18, 4.18
G17	11.16 (11.46)		7.31 (7.64)	5.93 (5.82)	2.52, 2.62 (2.35, 2.66)	4.73 (4.90)	4.13 (4.22)	4.19, 4.19
G18	10.60 (10.64)		7.65 (7.62)	6.14 (6.18)	2.47, 2.54 (2.49, 2.54)	4.95 (4.95)	4.05 (4.11)	3.94, 3.94 (3.91, .00)
T19		1.89 (1.92)	7.72 (7.73)	6.35 (6.34)	2.39, 2.51 (2.39, 2.50)	4.74 (4.75)	4.31 (4.38)	4.12, 4.15 (3.98, 4.18)
T20		2.01 (2.01)	7.78 (7.72)	6.43 (6.28)	2.45, 2.62 (2.25, 2.49)	4.94 (4.88)	4.35 (4.29)	3.96, 4.24
A21	8.44		8.57 (8.27)	6.72 (6.16)	2.59, 3.10 (2.70, 2.92)	5.08 (4.95)	4.51 (4.30)	4.00, 4.13 (3.72, 3.94)
G22	11.03 (11.60)		7.55 (7.12)	6.11 (5.87)	3.03, 3.60 (2.88, 3.20)	5.03 (4.88)	4.36 (4.37)	4.02, 3.95
G23	11.44 (11.41)		7.98 (7.87)	5.78 (5.75)	2.57, 2.65 (2.52, 2.63)	5.03 (5.00)	4.35 (4.30)	4.12, 4.12
G24	11.16 (11.28)		7.76 (7.74)	6.16 (6.15)	2.46, 2.65 (2.47, 2.72)	5.03 (4.90)	4.43 (4.44)	4.37, 4.37
T25		1.46 (1.41)	7.35 (7.27)	6.07 (6.04)	2.11, 2.38 (2.08, 2.37)	4.72 (4.76)	4.21 (4.20)	4.12, 4.12
T26		1.52 (1.50)	7.28 (7.25)	5.73 (5.70)	2.00, 1.99 (1.99, 1.99)	4.37 (4.36)	3.82 (3.81)	3.90, 4.02 (3.92, 4.04)

*Measured at 0 °C

** Assignments are not stereospecific

Table S2. Proton chemical shifts of wtTel26 in the 1:1 EPI-wtTel26 complex and the free wtTel26 in parentheses at 15 °C in pH 7, 100 mM K⁺.

Base	H1/H2/H3	HMe	H6/H8	H1'	H2', H2''	H3'	H4'	H5', H5'' **
T1	10.55*	1.39 (1.53)	7.02 (7.25)	5.62 (5.74)	1.43, 1.95 (1.82, 2.05)	4.19 (4.30)	3.71 (3.70)	4.08, 4.08 (3.49, 3.40)
T2	10.61*	0.70 (1.18)	7.06 (6.92)	5.63 (5.49)	1.95, 1.99 (1.64, 1.93)	4.53 (4.24)	3.79 (3.77)	3.54, 3.62 (3.21, 3.49)
A3	7.83		7.83 (7.95)	6.29 (6.00)	1.71, 2.32 (2.10, 2.52)	4.77 (4.65)	3.91 (4.02)	4.24, 4.24 (4.04, 3.62)
G4	11.59 (11.47)		7.41 (7.39)	5.96 (5.93)	2.90, 3.22 (2.90, 3.43)	4.77 (4.76)	4.19 (4.29)	3.91, 4.08 (4.09, 4.18)
G5	11.50 (11.69)		7.86 (7.83)	5.57 (5.64)	2.34, 2.47 (2.32, 2.58)	4.91 (4.90)	4.17 (4.17)	3.97, 4.07 (4.08, 4.23)
G6	10.86 (10.78)		7.68 (7.64)	5.82 (5.85)	2.21, 2.34 (2.21, 2.24)	4.83 (4.86)	4.24 (4.26)	4.04, 4.04 (3.94, 4.08)
T7		1.67 (1.72)	7.48 (7.57)	6.06 (6.11)	1.99, 2.33 (2.05, 2.40)	4.58 (4.60)	4.19 (4.21)	4.02, 4.08 (3.78, 4.10)
T8		1.59 (1.64)	7.26 (7.32)	5.56 (5.66)	1.78, 2.00 (1.82, 2.05)	4.37 (4.46)	3.84 (3.88)	3.73, 3.84 (3.42, 3.82)
A9	7.32 (7.48)		7.56 (7.68)	5.59 (5.67)	1.88, 2.36 (1.85, 2.34)	4.82 (4.79)	4.03 (4.01)	3.84, 3.97 (3.97, 3.91)
G10	10.93 (11.02)		7.11 (7.20)	5.85 (5.94)	3.49, 2.93 (3.61, 3.05)	4.53 (4.72)	4.17 (4.29)	4.01, 4.08 (4.17, 4.05)
G11	10.76 (10.96)		7.26 (7.27)	5.60 (5.65)	2.45, 2.32 (2.44, 2.33)	4.82 (4.88)	4.00 (4.09)	4.06, 4.21 (4.03, 4.20)
G12	11.42 (11.47)		7.66 (7.62)	5.58 (5.79)	2.38, 2.55 (2.25, 2.45)	4.90 (4.93)	4.20 (4.24)	3.94, 4.10 (3.99, 4.03)
T13	12.57	1.44 (1.78)	7.09 (7.60)	5.69 (5.97)	1.89, 2.56 (2.15, 2.45)	4.84 (4.74)	4.02 (4.27)	4.04, 4.04 (3.87, 4.09)
T14	10.46*	1.68 (1.55)	7.63 (7.28)	5.75 (5.81)	2.34, 2.85 (1.59, 1.99)	4.90 (4.63)	4.03 (4.08)	3.81, 3.81 (4.02, 3.87)
A15	7.89		8.33 (7.99)	6.31 (6.32)	2.14, 2.84 (2.67, 2.67)	4.75 (4.90)	4.21 (4.33)	4.02, 4.14 (4.17, 4.06)
G16	10.54 (11.06)		7.44 (7.00)	6.03 (5.85)	2.93, 3.48 (2.84, 3.33)	4.61 (4.85)	4.23 (4.35)	4.13, 4.13 (4.24, 4.17)
G17	11.05 (11.34)		7.20 (7.52)	5.82 (5.72)	2.42, 2.49 (2.24, 2.57)	4.69 (4.80)	4.08 (4.11)	4.05, 4.05 (3.77, 4.24)
G18	10.47 (10.49)		7.56 (7.52)	6.03 (6.05)	2.38, 2.42 (2.36, 2.45)	4.82 (4.86)	3.96 (3.92)	3.83, 3.92 (3.87, 3.93)
T19		1.76 (1.82)	7.61 (7.67)	6.24 (6.27)	2.25, 2.38 (2.28, 2.39)	4.63 (4.62)	4.27 (4.32)	3.97, 4.02 (4.01, 4.08)
T20		1.90 (1.93)	7.68 (7.71)	6.33 (6.24)	2.35, 2.53 (2.26, 2.45)	4.82 (4.81)	4.26 (4.19)	3.85, 4.14 (3.75, 4.07)
A21	8.33		8.47 (8.16)	6.62 (6.12)	2.48, 2.99 (2.67, 2.83)	4.97 (4.91)	4.40 (4.26)	3.86, 4.01 (4.22, 3.89)
G22	10.94 (11.48)		7.44 (7.03)	6.02 (5.74)	2.93, 3.49 (2.77, 2.95)	4.90 (4.72)	4.26 (4.28)	3.84, 3.93 (4.06, 4.22)
G23	11.32 (11.30)		7.89 (7.80)	5.67 (5.66)	2.47, 2.55 (2.45, 2.57)	4.92 (4.90)	4.24 (4.21)	4.14, 4.20 (4.07, 4.13)
G24	11.06 (11.18)		7.66 (7.69)	6.05 (6.04)	2.34, 2.56 (2.39, 2.59)	4.92 (4.79)	4.33 (4.34)	3.92, 4.23 (3.98, 4.12)
T25		1.31 (1.30)	7.23 (7.24)	5.94 (5.96)	1.99, 2.27 (1.98, 2.29)	4.62 (4.63)	4.08 (4.11)	3.95, 4.07 (3.81, 4.10)
T26		1.37 (1.38)	7.13 (7.14)	5.54 (5.55)	1.84, 1.84 (1.85, 1.85)	4.23 (4.25)	3.68 (3.68)	3.79, 3.92 (3.93)

* Measured at 0 °C

** Assignments are not stereospecific

Table S3. Proton chemical shifts of EPI in the 1:1 EPI-wtTel26 complex and in the free EPI (in parentheses) at 25 °C in pH 7, 100 mM K⁺.

Proton	Complex (Free)
HA	3.49 (3.88)
HB	3.57 (3.90)
H1	6.81 (7.29)
H4	6.39 (6.93)
H51	2.44 (3.18)
H52	2.83 (3.18)
H61	4.90 (4.76)
H62	4.90 (4.76)
H8	6.81 (9.49)
H11	5.88 (7.76)
H12	5.52 (7.63)
H13	7.87 (8.35)
HC1	6.25 (6.40)
HC2	6.16 (6.40)

Table S4A. Interresidue NOEs between the 5'-external G-tetrad and the EPI-A3 plane.

		G4		G12					G16			G22			
		H1	H22	H1	H8	H1'	H2'	H2''	H3'	H1	H8	H22	H1	H8	H22
EPI	H12										M				
	H13	w								M					
	H1			w	w					M					
	H4			M							w				
	H8	M		M						w			M		
	HA				M	w	M	M	M	M		M			
	HB				w	M	w	w	w						
	H51	M		M											
	H52	w		M											
	H6	M		M											
	HC1												M		w
	HC2												M		M
A3	H2	w		w											
	H1'	M	M											M	
	H2''	w	w												

M = Medium intensity, w = weak intensity

Table S4B. Interresidue NOEs between EPI and A3.

		A3	
		H2	NH6
EPI	H4	M	
	H8	M	M
	H51	S	
	H52	M	
	H6	S	
	HC1		M
	HC2		S

S = Strong intensity, M = Medium intensity

Table S5A. Interresidue NOEs between the EPI-A3 plane and the T2-T13-A15 triad and A21.

		T13				A15				T2				A21			
		H3	HMe	H6	H5',''	H2	H8	H2'	H2''	HMe	H6	H1'	H2'	H2''	H2	H8	H1'
EPI	H11						M										
	H12					w		M	M								
	H13	M															
	H1	M				w											
	H4		S	M													
	HA	M	M	M	M	w											
	HB	w	S	S	M												
	H51		M														
	H52		M														
	H6		w														
	HC1									w						w	w
	HC2									w					w	M	w
A3	H2		M							w	M						
	H8									w	M	M	M	M			
	NH6	M								M	M	w	w	w			

S = Strong intensity, M = Medium intensity, w = weak intensity

Table S5B. Interresidue NOEs of the T2-T13-A15 capping triad.

		T13			A15	
		H3	HMe	H6	H2	H1'
T2	H3				M	
	HMe					M
T13	H3	/	/	/	S	

S = Strong intensity, M = Medium intensity

Table S6. Interresidue NOEs between the T2-T13-A15 triad and the T1-T14 pair.

		T2		T13		A15	
		H3	HMe	H3	H6	H2	H1'
T1	HMe	M	w				
	H6		M				
	H2'		w				
	H2''		M				
T14	HMe			w	M		
	H6				w		
	H1'					M	
	H2'					M	M
	H2''					M	

M = Medium intensity, w = weak intensity

Table S7. Distance constraints and structure statistics for the 1:1 EPI-wtTel26 complex in K⁺.

NMR distance constraints	
Total NOEs:	631
Intra-residue restraints:	352
Inter-residue restraints:	217
Inter EPI-DNA restraints:	62
Hydrogen Bonds:	33
Structure Statistics	
NOE violations	
Mean number (>0.2 Å)	0.0
R.m.s.d. of violations (Å)	0.014 ± 0.002
Pairwise r.m.s.d. of heavy atoms (Å)	
G-tetrads	0.99 ± 0.19
Binding Pocket	1.04 ± 0.18
(T1-G4, G12-G16, G22, EPI)	
Ordered Regions	1.30 ± 0.22
(Omitting T7, T19-A21 loops)	
Backbone	1.83 ± 0.32
All heavy atoms	1.89 ± 0.33

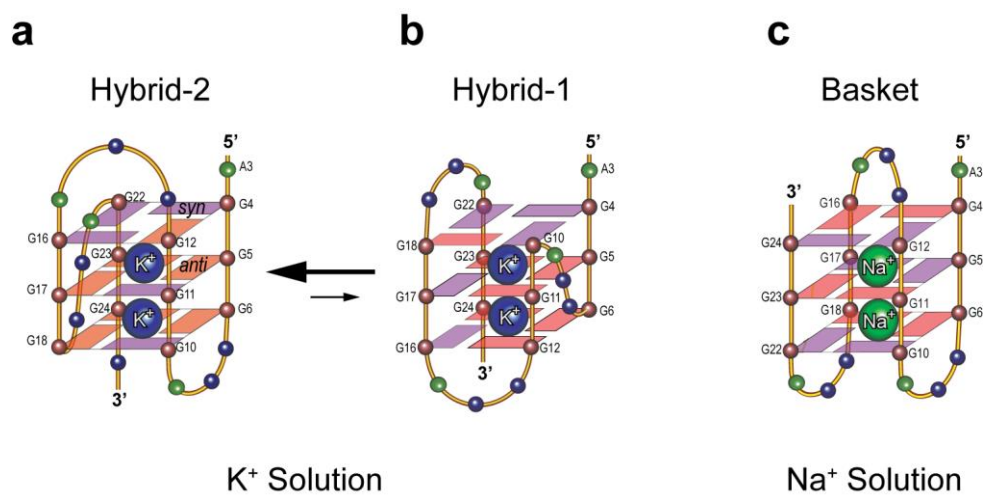


Figure S1. Wild-type human telomeric sequences form a mixture of hybrid-2 G-quadruplex (a) and hybrid-1 G-quadruplex (b) in K^+ solution, with hybrid-2 being the major conformation, and basket-type G-quadruplex in Na^+ solution (c).

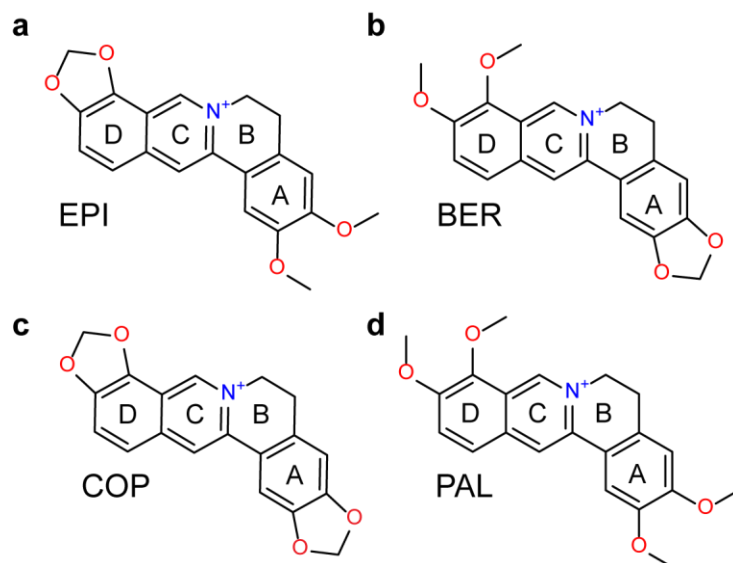


Figure S2. Chemical structures of protoberberine alkaloids epiberberine (EPI) (a), berberine (BER) (b), coptisine (COP) (c), and palmatine (PAL) (d). These compounds contain the same pharmacophore with different combination of methylenedioxy moiety vs two methoxy groups at the two ends.

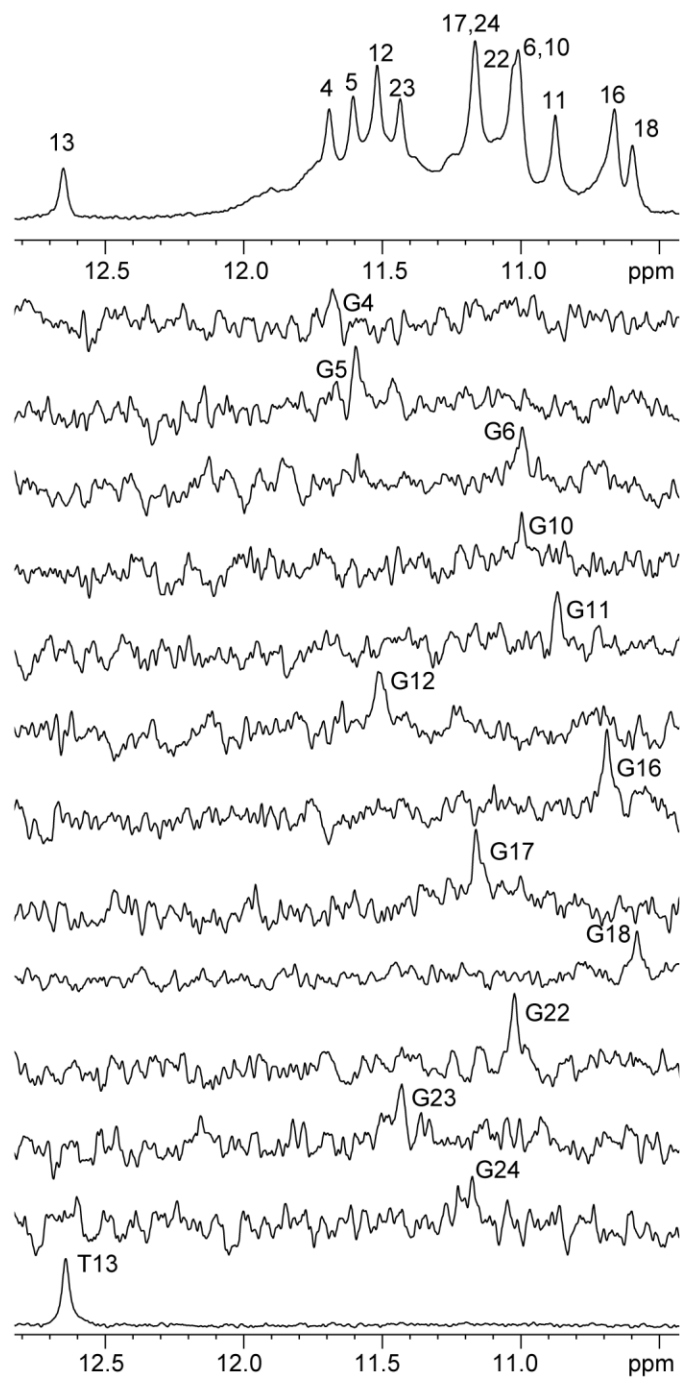


Figure S3. Imino proton assignment for the 1:1 EPI-wtTel26 complex obtained by ^{15}N -edited HMQC experiments using site-specific-labeled wtTel26 DNA. The assignments for the guanine imino protons are shown in the top spectra; the assignment for the T13 imino proton is shown in the bottom spectrum. Conditions: 25°C, pH 7, 100 mM K^+ .

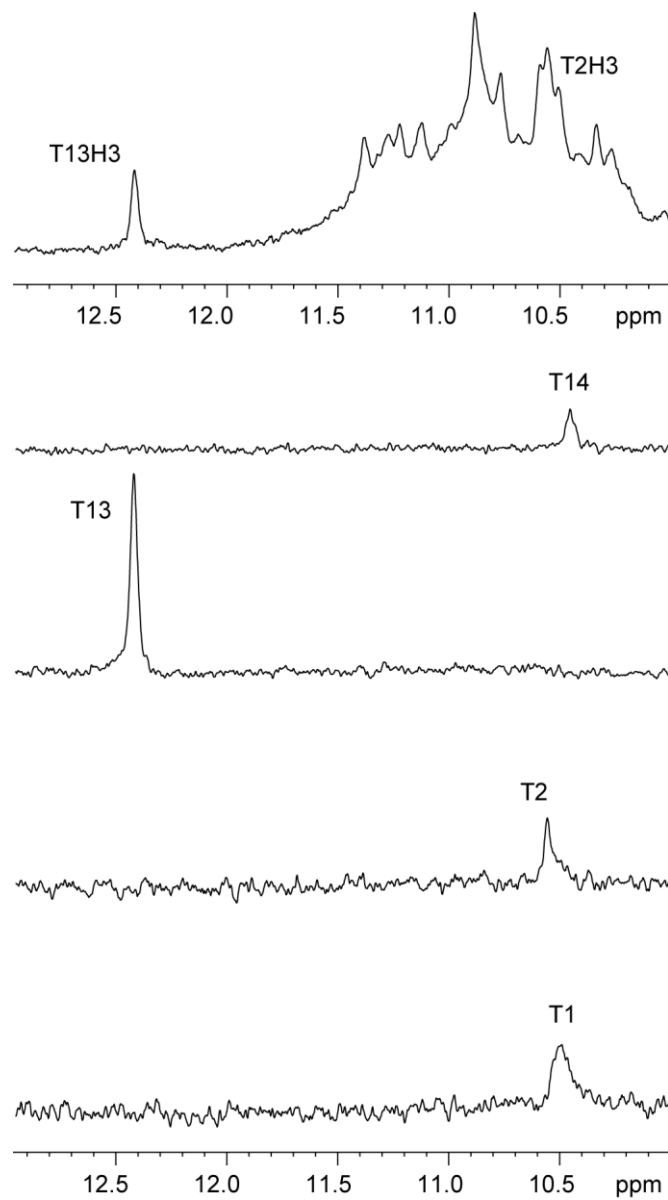


Figure S4. The assignment of thymine imino protons for the 1:1 EPI-wtTel26 complex using 1D ¹⁵N-edited HMQC experiments on site-specific-labeled wtTel26 DNA. Conditions: 0 °C, pH 7, 100 mM K⁺.

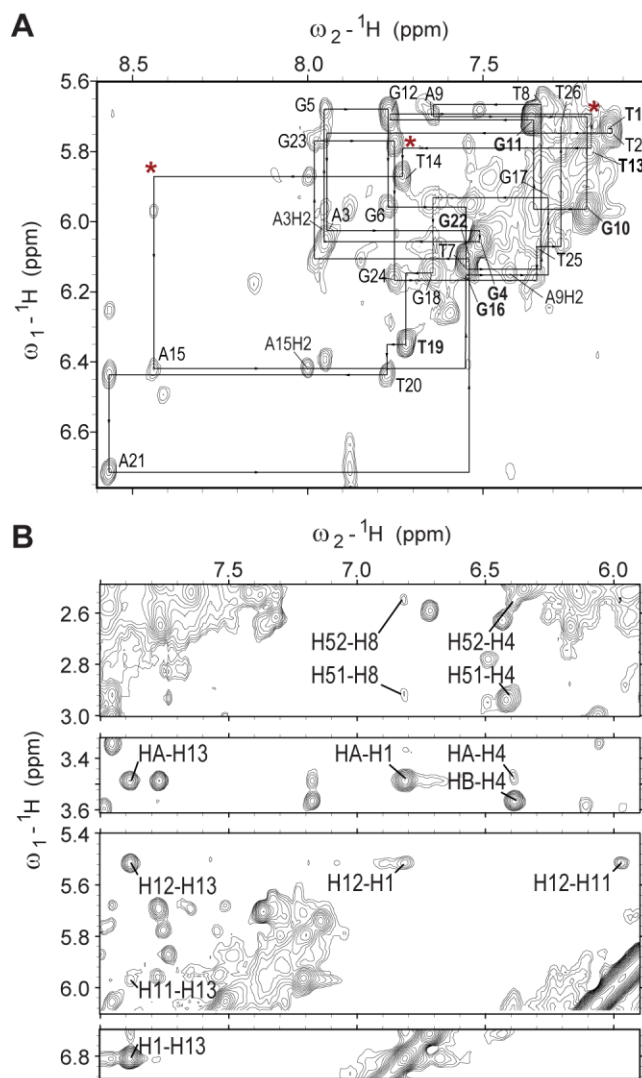


Figure S5. (a) The expanded aromatic-H1' region of the 2D-NOESY spectrum of the 1:1 EPI-wtTel26 complex. The sequential assignment pathways are shown for the DNA strand (T₁-T₂₆). The interruptions of NOE connectivity by EPI binding are labeled with red asterisks. The *syn* residues are in bold. (b) Expanded aromatic regions of the 2D-NOESY spectrum of the 1:1 EPI-wtTel26 complex. Assignments are shown for the intra-EPI NOEs. Conditions: 25 °C, pH 7, 100 mM K⁺.

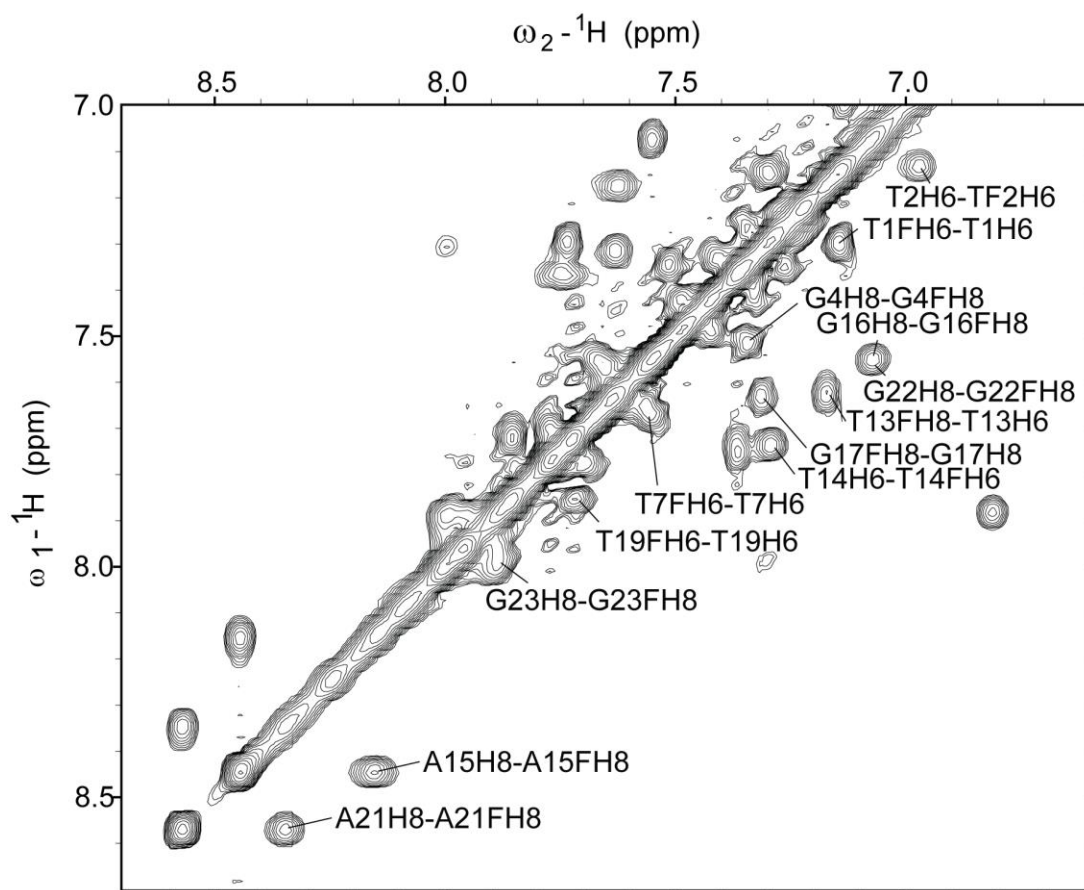


Figure S6. Expanded aromatic-aromatic region of the 2D-NOESY spectrum of the 0.75:1 EPI-wtTel26 complex. Assignments are shown for the observed exchange peaks between the free and bound wtTel26 DNA. Conditions: 25 °C, pH 7, 100 mM K⁺.

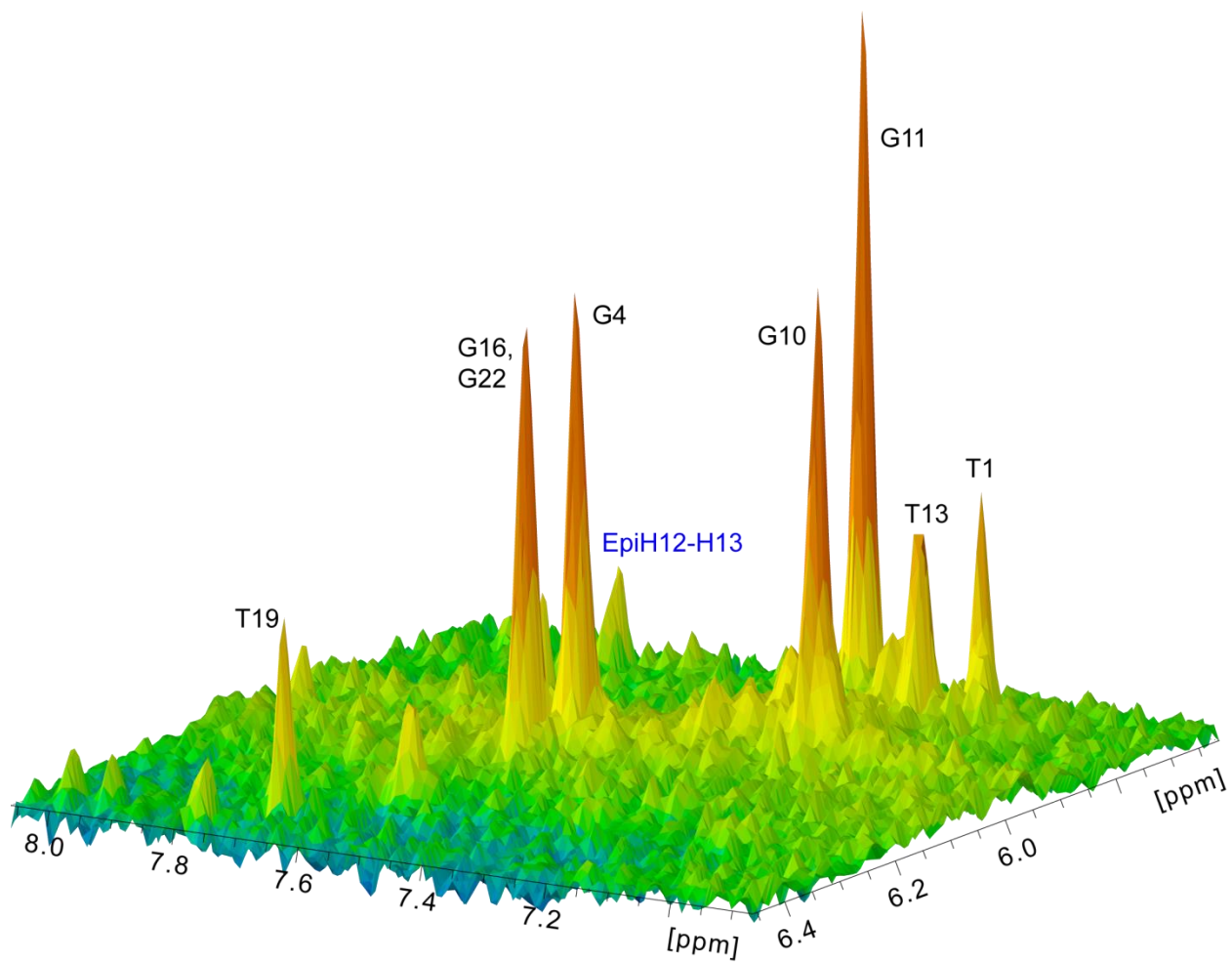


Figure S7. Stacked plot of the 2D NOESY spectrum with 50 ms mixing time showing intra-residue H1'-H6 and H1'-H8 cross-peaks of *syn*-configuration DNA residues. The observed intra-EPI peak is labeled in blue. Conditions: 25 °C, pH 7, 100 mM K⁺.

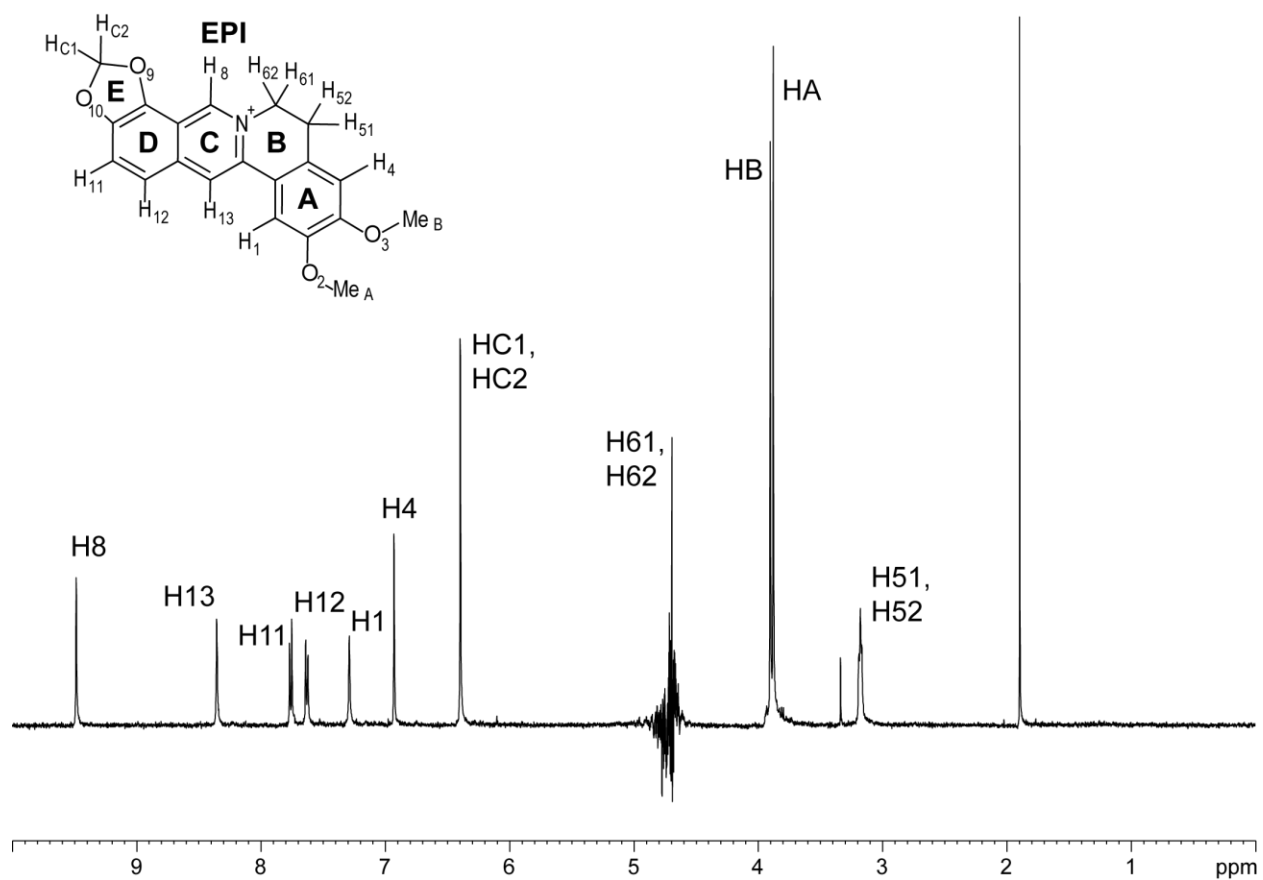


Figure S8a. 1D ¹H NMR spectrum of the free EPI in pH 7, 100 mM K⁺ at 25 °C with peak assignments and corresponding schematic structure.

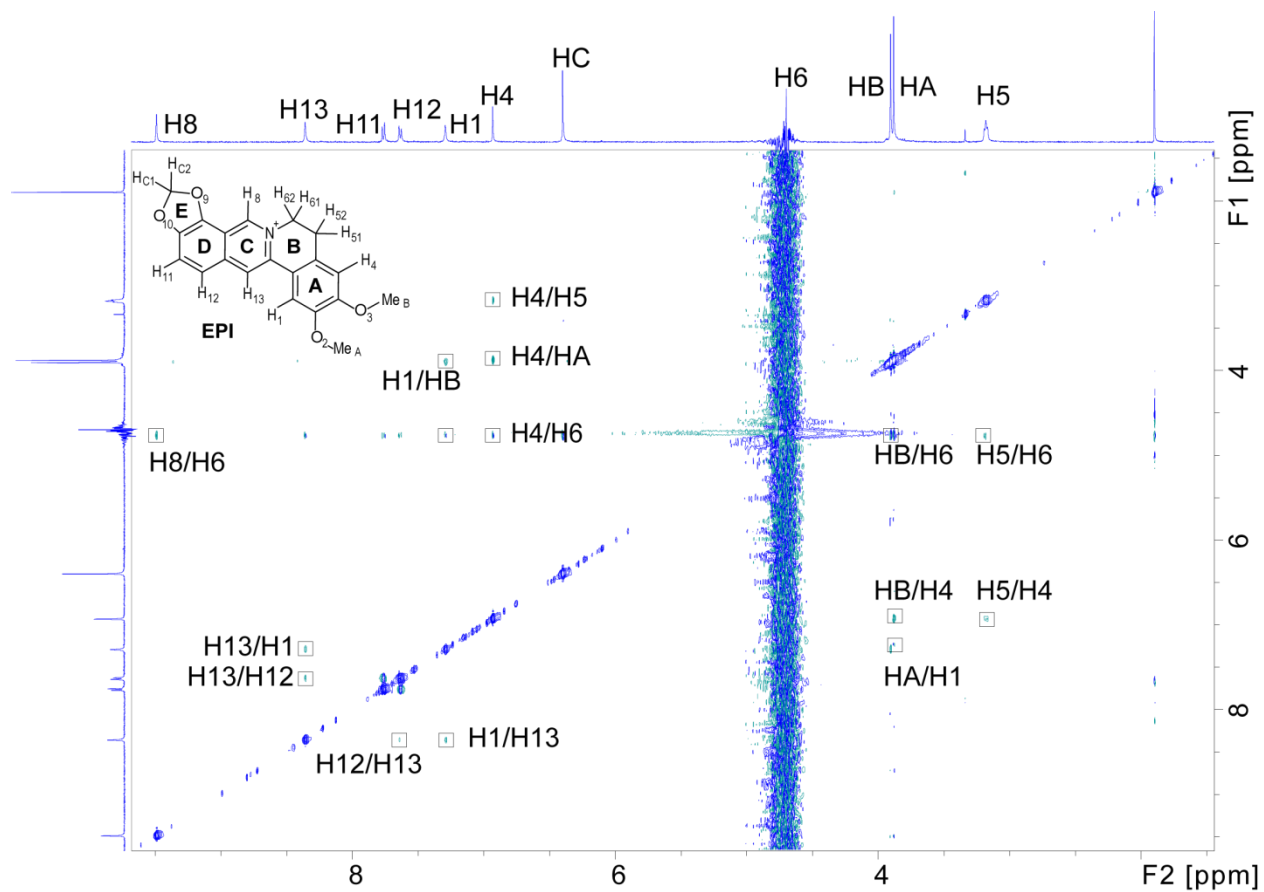


Figure S8b. 2D NOESY spectrum of the free EPI in pH 7, 100 mM K⁺ at 25 °C with peak assignments and corresponding schematic structure.

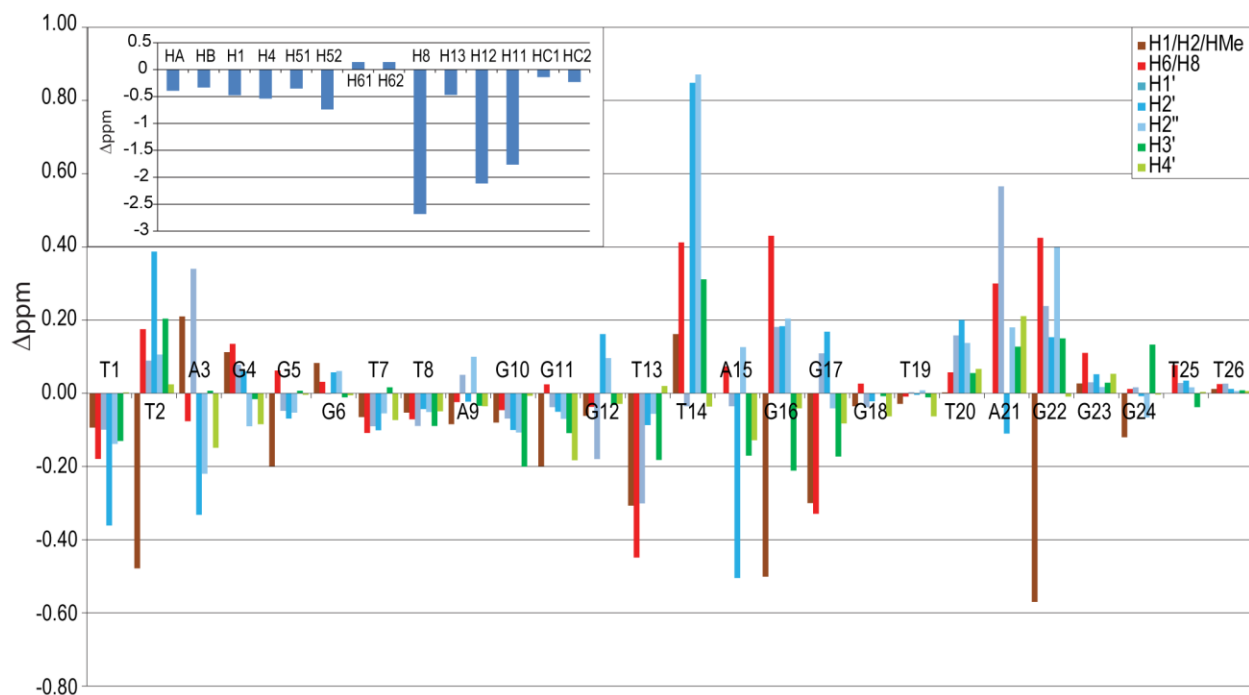


Figure S9. The proton chemical shift differences between the bound (in 1:1 EPI-wtTel26 complex) and free wtTel26 in pH 7, 100 mM K^+ at 25 °C. (Inset) The proton chemical shift differences between the bound and free EPI at 25 °C.

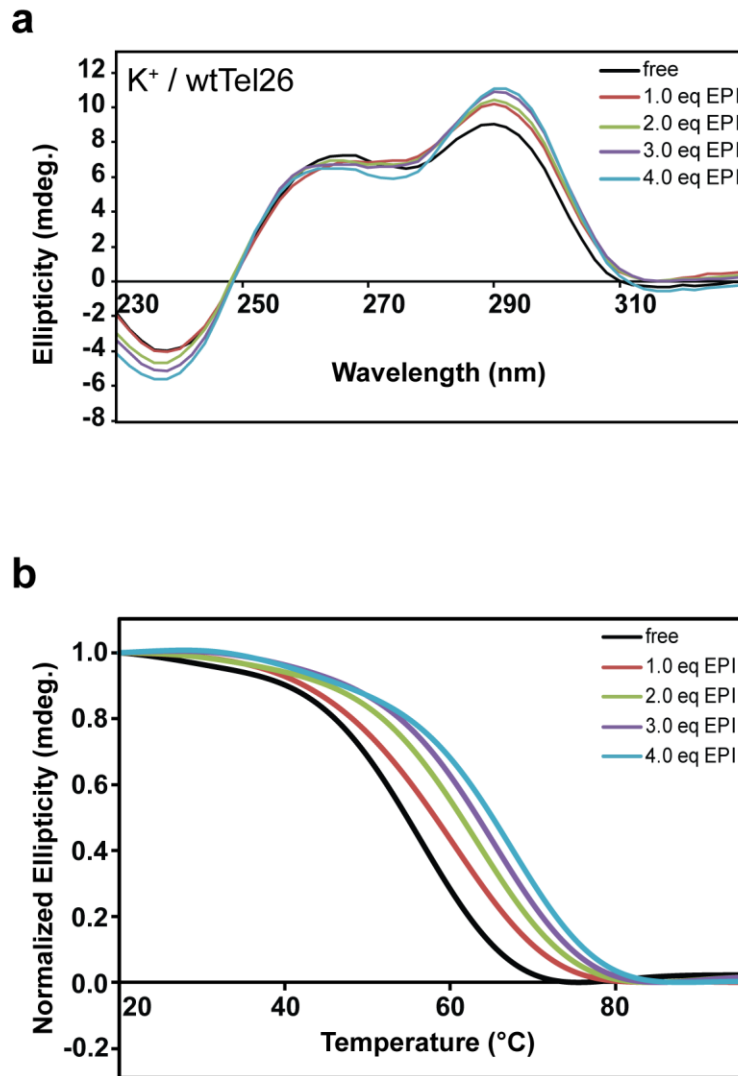


Figure S10. CD spectra (a) and CD thermal melting curves (b) of wtTel26 with addition of EPI at 1, 2, 3, and 4 equivalents in pH 7, 100 mM K^+ solution.

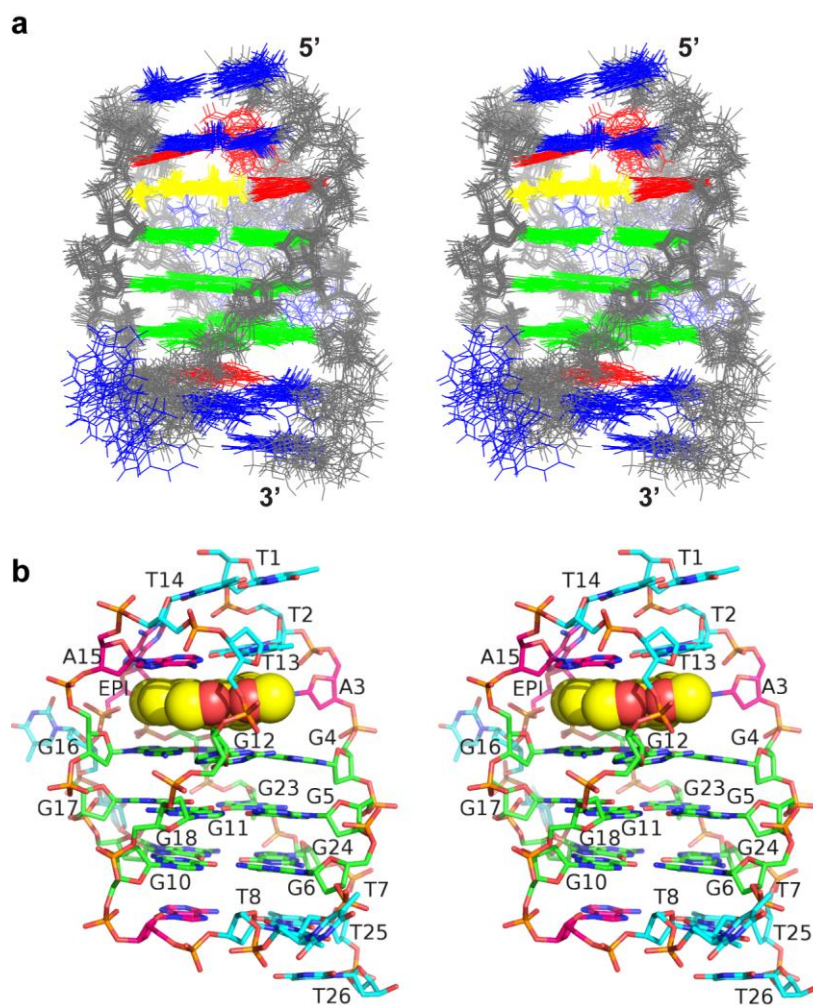


Figure S11. (a) Stereo view of superimposed 15 final NMR structures of the 1:1 wtTel26-EPI complex. Guanine bases are shown in green, adenine in red, thymine in blue, and EPI in yellow. (b) Stereo view of the representative NMR structure of the 1:1 wtTel26-EPI complex. EPI is shown in yellow CPK model, guanines in green, adenines in magenta, and thymines in cyan.

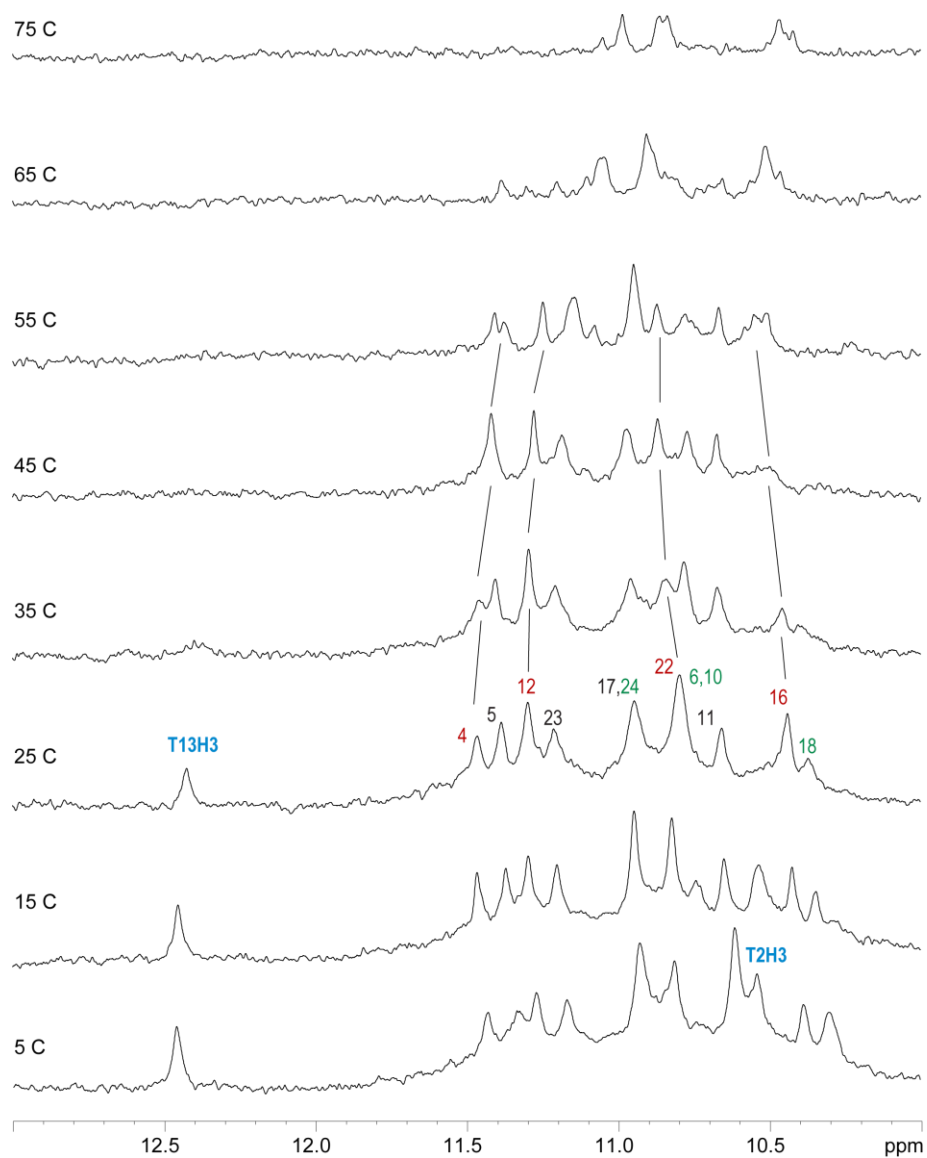


Figure S12. The imino proton regions of the variable temperature ^1H NMR spectra of the 1:1 wtTel26-EPI complex in pH 7, 100 mM K^+ . Assignments are shown at 25 $^\circ\text{C}$. The guanine imino protons of the 5'-external G-tetrad are in red, the middle G-tetrad in black, and the 3'-external G-tetrad in green. The thymine imino protons are labeled in cyan.

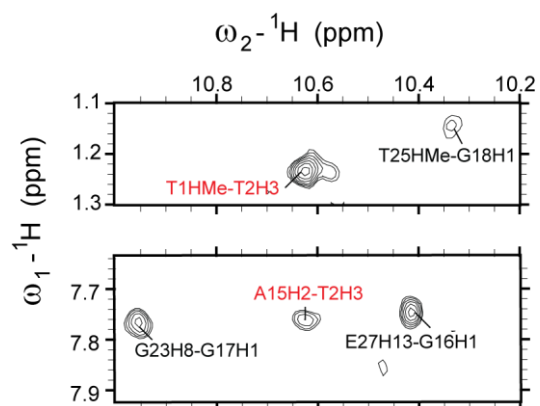


Figure S13. Expanded imino regions of the 2D-NOESY spectrum of the 1:1 EPI-wtTel26 complex with NOE cross-peaks of T2/H3 colored in red. Conditions: 5 °C, pH 7, 100 mM K⁺.

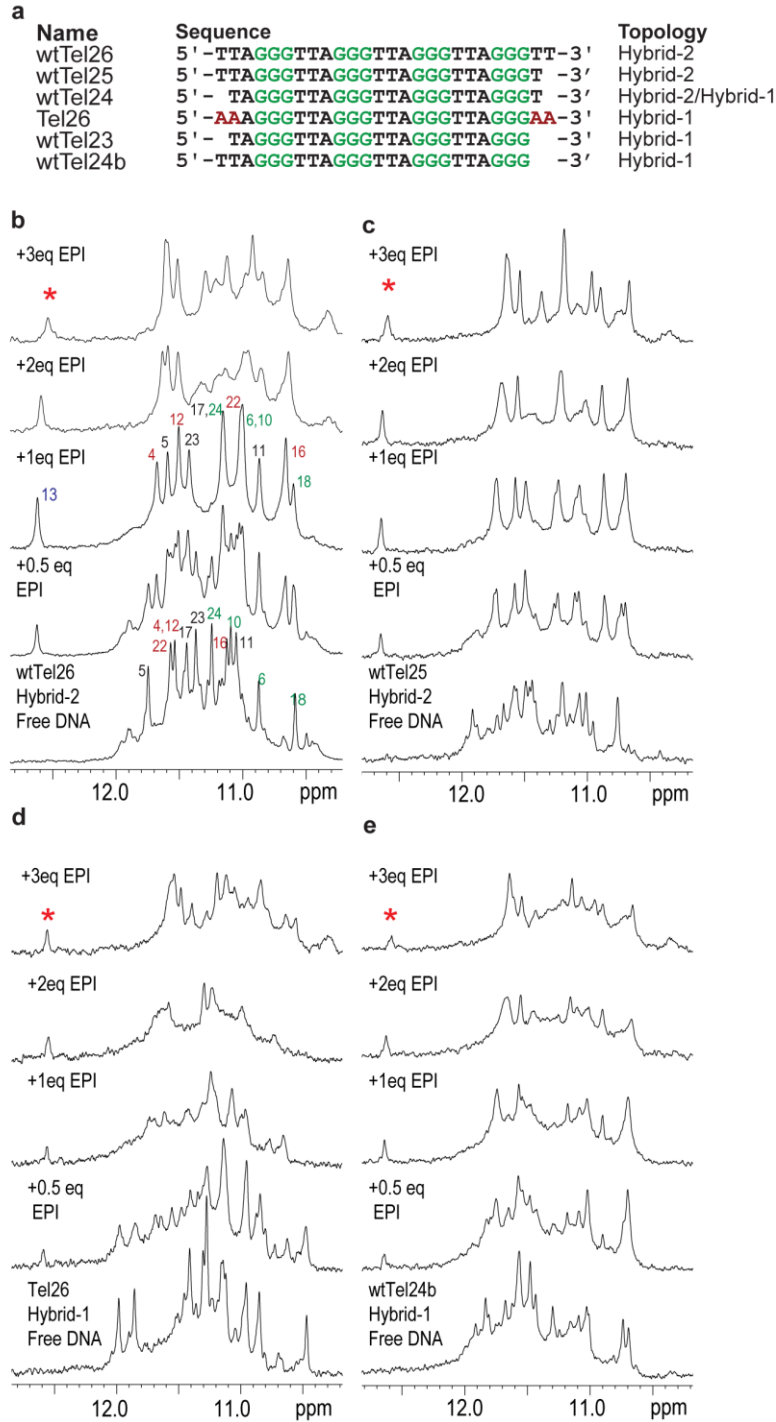


Figure S14. (a) Human telomeric DNA sequences with their folding topologies observed in K^+ solution. Wild-type human telomeric sequences are named wtTel, with numbers indicating the sizes of the DNA. (b-e) The imino regions of the 1H NMR titration of EPI with wtTel26 (hybrid-2) (b), wtTel25 (hybrid-2) (c), Tel26 (hybrid-1) (d), and wtTel24b (hybrid-1) (e). A signature thymine imino proton resonance at 12.6 ppm is observed in all sequences and is labeled with red asterisk. Conditions: 25 °C, pH 7, 100 mM K^+ .

a Name	Sequence	Topology
MycG4	5' -TGAGGGTGGGTAGGGTGGGTAA-3'	Parallel
BCL2Mid	5' -GGCGCGGGAGGAATTGGCGGG-3'	Hybrid-2
PDGFR-β 5'Mid	5' -AAGGGAGGGCGGCGGGCAGGG-3'	Parallel

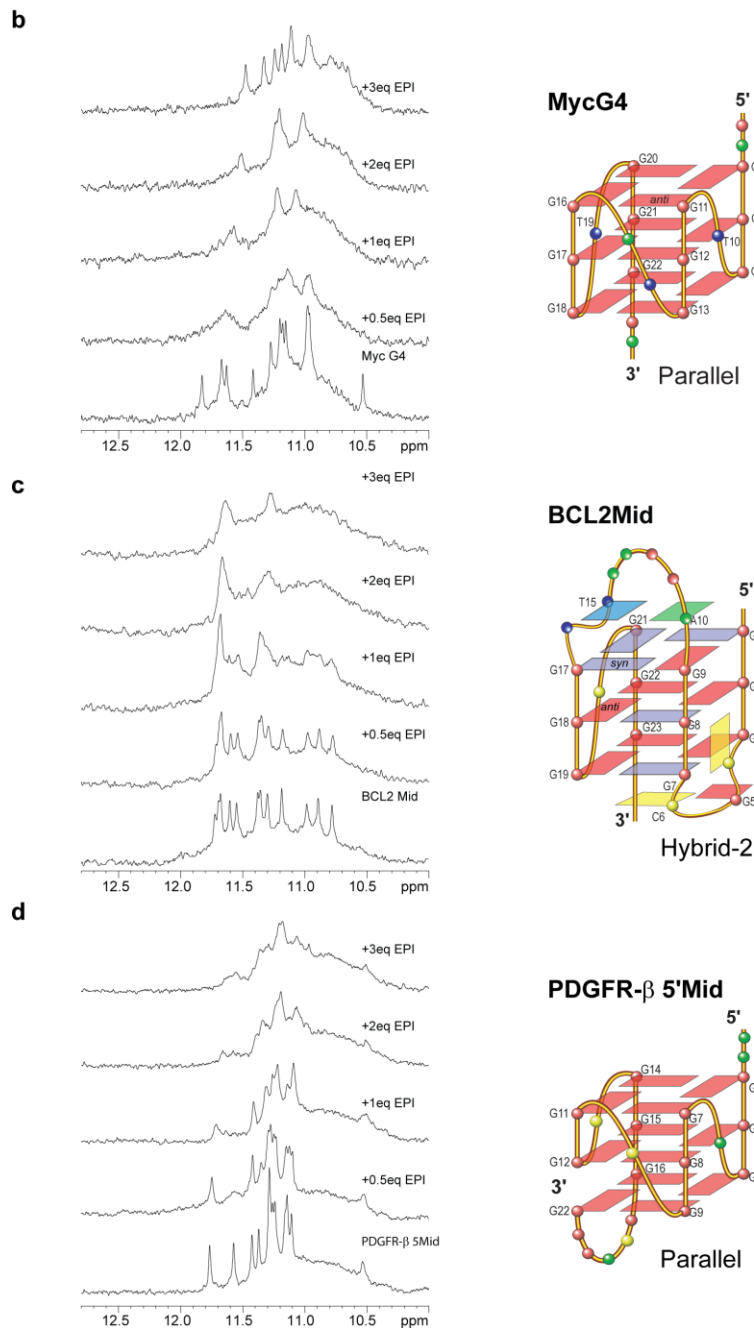


Figure S15. (a) Human promoter DNA sequences with known G-quadruplex structures in K^+ solution. (b-d) The imino regions of the 1H NMR titration of EPI with various DNA G-quadruplexes in K^+ solution, including c-MYC promoter G4 MycG4^[7] (b), BCL2 promoter G4 BCL2Mid^[8] (c), and PDGFR-β promoter G4 PDGFR-β 5'Mid^[9](d). G-quadruplex folding schematics are depicted to the right. Conditions: 25 °C, pH 7, 100 mM K^+ .

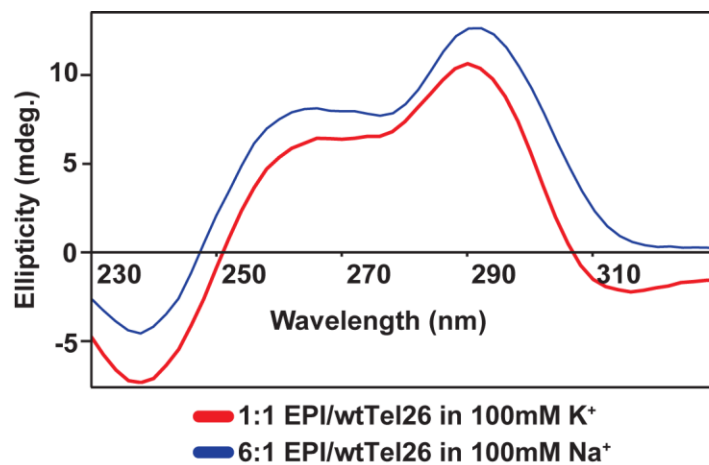


Figure S16. The saturated CD spectrum of the 6:1 EPI-wtTel26 complex in Na⁺ solution closely resembles that of the 1:1 EPI-wtTel26 hybrid-2 complex in K⁺ solution, suggesting the formation of the hybrid-2 structure.

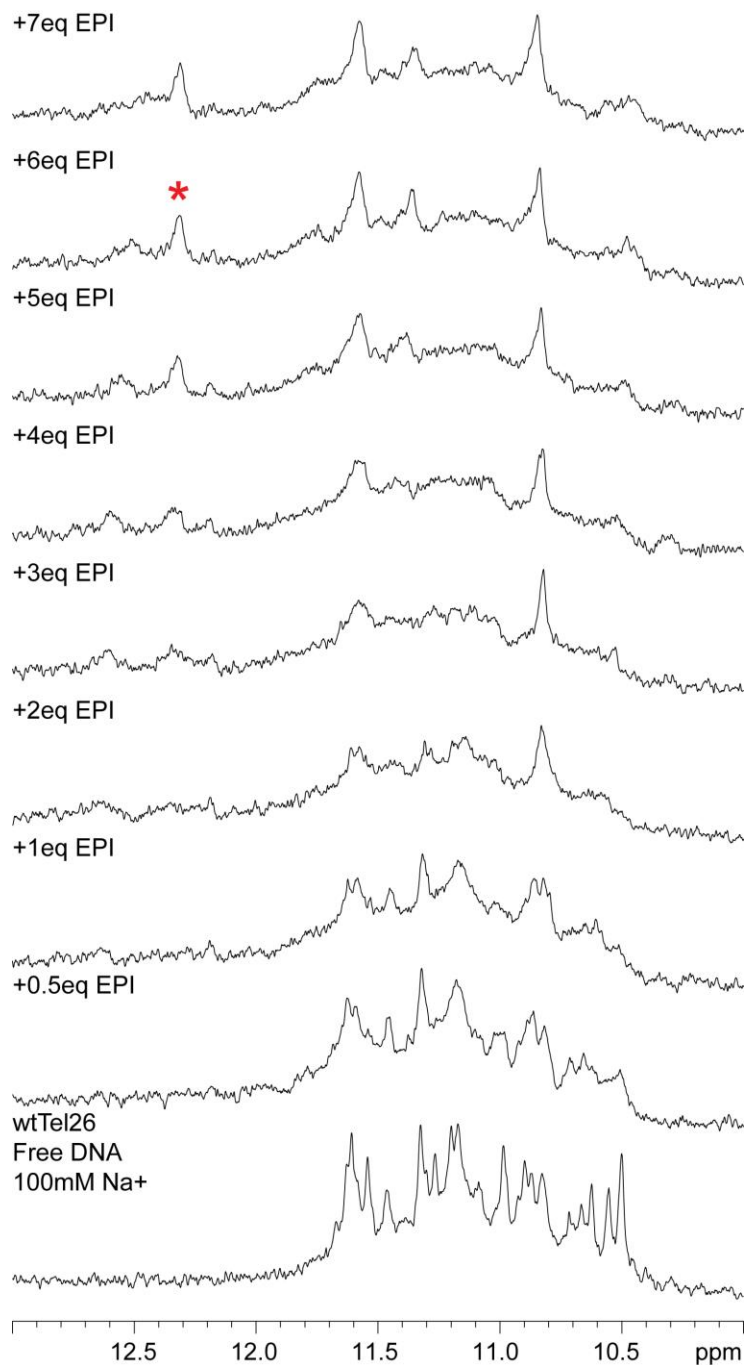
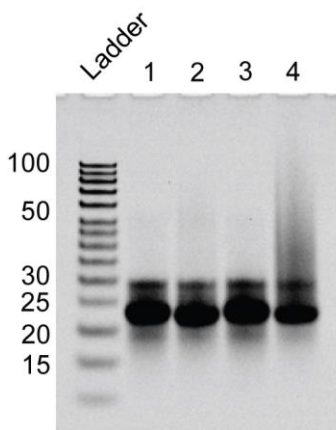


Figure S17. 1D ¹H NMR titration of EPI to wtTel26 in 100 mM Na⁺, pH 7, 25 °C. The signature thymine imino resonance is labeled with red asterisk. Proton resonances were slightly shifted in Na⁺ solution, with the signature imino peak of the EPI-hybrid-2 complex observed at 12.4 ppm.



1. Free wtTel26 in Na⁺
2. 7:1 EPI - wtTel26 in Na⁺
3. Free wtTel26 in K⁺
4. 4:1 EPI - wtTel26 in K⁺

Figure S18. Native EMSA gel of free wtTel26 and 7:1 EPI-wtTel26 in 100 mM Na⁺, and free wtTel26 and 4:1 EPI-wtTel26 in 100 mM K⁺.

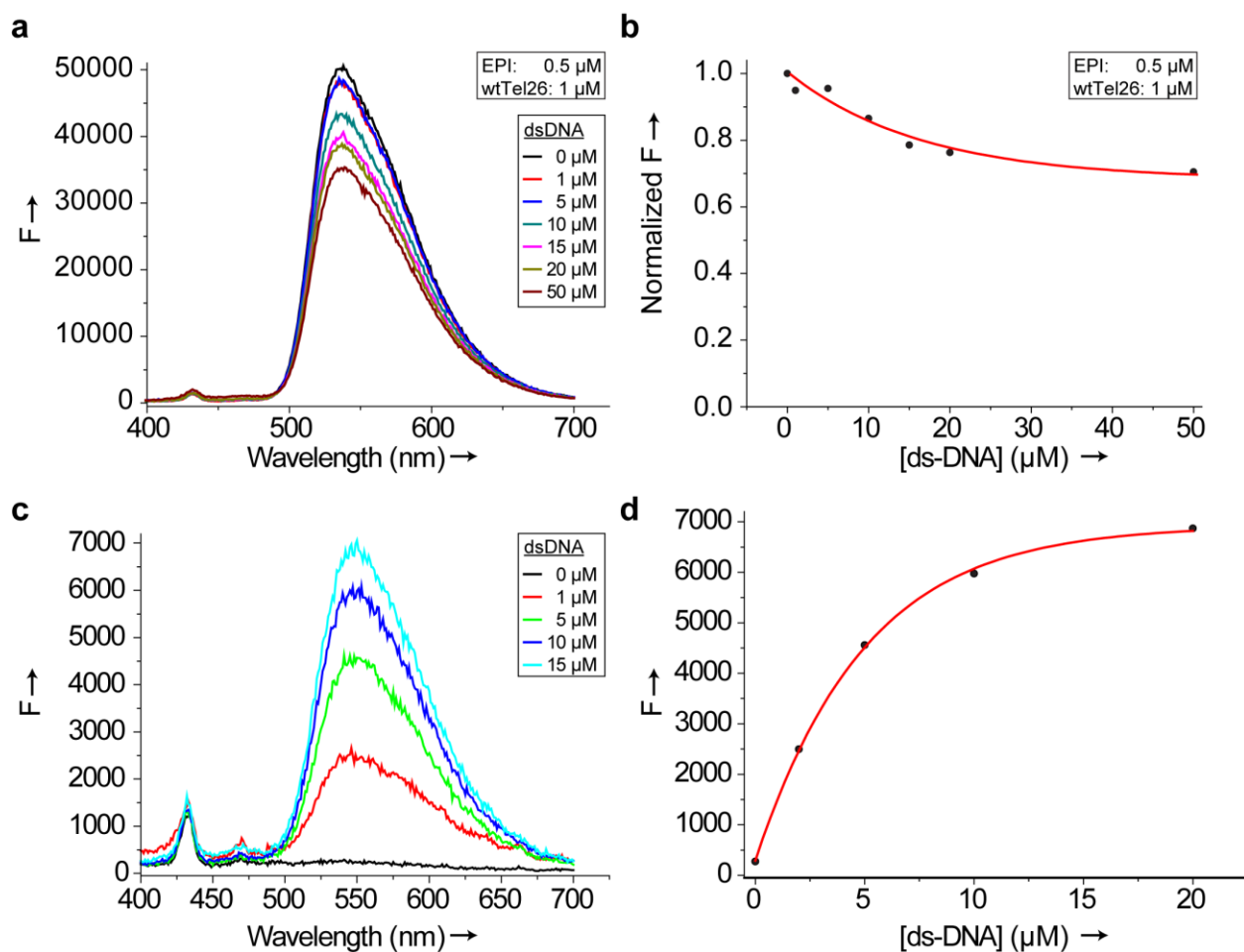


Figure S19. (a-b) Fluorescence competition experiments of EPI binding with human telomeric DNA wtTel26 G4 and dsDNA (5'-GTGTTGACAGCAGCG : 5'-CGCTGCTGTCAACAC) in pH 7 (PBS), 100 mM K⁺. Fluorescence emission spectra (a) and the normalized fluorescence (b) of 0.5 μM EPI in complex with 1 μM wtTel26 titrated with increasing amount of the dsDNA. (c-d) Fluorescence measurement of the binding of EPI (0.5 μM) to the dsDNA in pH 7 (PBS), 100 mM K⁺. Fluorescence emission spectra of EPI upon titration of the dsDNA (c) and fluorescence intensity at increasing dsDNA concentration (d). The apparent K_a of EPI binding to dsDNA is estimated to be $(2.19 \pm 0.21) \times 10^5 \text{ M}^{-1}$. The binding of EPI to human telomeric G-quadruplexes in 100 mM K⁺ was reported to be $\sim 2.8 \times 10^7 \text{ M}^{-1}$.^[6]

REFERENCES

- [1] a) A. Ambrus, D. Chen, J. Dai, T. Bialis, R. A. Jones, D. Yang, *Nucleic Acids Res* **2006**, *34*, 2723-2735; b) J. X. Dai, M. Carver, C. Punchihewa, R. A. Jones, D. Z. Yang, *Nucleic Acids Res* **2007**, *35*, 4927-4940; c) J. Dai, M. Carver, L. H. Hurley, D. Yang, *J Am Chem Soc* **2011**, *133*, 17673-17680.
- [2] a) A. T. Phan, D. J. Patel, *J Am Chem Soc* **2002**, *124*, 1160-1161; b) A. A. Szewczak, G. W. Kellogg, P. B. Moore, *Febs Letters* **1993**, *327*, 261-264.
- [3] A. T. Brünger, *X-PLOR: version 3.1: a system for x-ray crystallography and NMR*, Yale University Press, **1992**.
- [4] A. W. Schuëttelkopf, D. M. Van Aalten, *Acta Crystallogr Sect D: Biol Crystallogr* **2004**, *60*, 1355-1363.
- [5] H. Han, L. H. Hurley, M. Salazar, *Nucleic Acids Res* **1999**, *27*, 537-542.
- [6] L. Zhang, H. Liu, Y. Shao, C. Lin, H. Jia, G. Chen, D. Yang, Y. Wang, *Anal Chem* **2015**, *87*, 730-737.
- [7] A. Ambrus, D. Chen, J. Dai, R. A. Jones, D. Yang, *Biochem* **2005**, *44*, 2048-2058.
- [8] J. Dai, T. S. Dexheimer, D. Chen, M. Carver, A. Ambrus, R. A. Jones, D. Yang, *J Am Chem Soc* **2006**, *128*, 1096-1098.
- [9] Y. Chen, P. Agrawal, R. V. Brown, E. Hatzakis, L. Hurley, D. Yang, *J Am Chem Soc* **2012**, *134*, 13220-13223.